

Published in final edited form as:

Chem. 2024 May 9; 10(5): 1528–1540. doi:10.1016/j.chempr.2024.02.001.

A prebiotic Krebs cycle analog generates amino acids with H₂ and NH₃ over nickel

Harpreet Kaur^{#1}, Sophia A. Rauscher^{#1}, Emilie Werner¹, Youngdong Song², Jing Yi¹, Wahnyalo Kazöne¹, William F. Martin³, Harun Tüysüz², Joseph Moran^{1,4,5,7,*}

¹Institut de Science et d'Ingénierie Supramoléculaires (ISIS), CNRS UMR 7006, Université de Strasbourg, 8 allée Gaspard Monge, 67000 Strasbourg, France

²Max-Planck-Institut für Kohlenforschung, Kaiser-Wilhelm-Platz 1, 45470 Mülheim an der Ruhr, Germany

³Institute for Molecular Evolution, Heinrich-Heine-University of Düsseldorf, Universitätsstr. 1, 40225 Düsseldorf, Germany

⁴Institut Universitaire de France, 75005 Paris, France

⁵Department of Chemistry and Biomolecular Sciences, University of Ottawa, Ottawa, Ontario K1N 6N5, Canada

These authors contributed equally to this work.

Summary

Hydrogen (H₂) has powered microbial metabolism for roughly 4 billion years. The recent discovery that it also fuels geochemical analogs of the most ancient biological carbon fixation pathway sheds light on the origin of metabolism. However, it remains unclear whether H₂ can sustain more complex nonenzymatic reaction networks. Here, we show that H₂ drives the nonenzymatic reductive amination of six biological ketoacids and glyoxylate to give the corresponding amino acids in good yields using ammonium concentrations ranging from 6 to 150 mM. Catalytic amounts of nickel or ground meteorites enable these reactions at 22°C and pH 8. The same conditions promote an H₂-dependent ketoacid-forming reductive aldol chemistry that co-occurs with reductive amination, producing a continuous reaction network resembling amino acid synthesis in the metabolic core of ancient microbes. The results support the hypothesis that the earliest biochemical networks could have emerged without enzymes or RNA.

Abstract

Author Contributions

J.M. conceived the research. H.K., S.A.R., E.W., and J.Y. performed the experiments, under supervision from J.M. Y.S. synthesized and characterized the catalysts, under supervision from H.T. W.K. developed analytical protocols. J.M., H.K., and E.W. wrote the paper, with feedback from all authors. H.K., S.A.R., E.W., and Y.S. assembled the supplementary information.

This is an open access article under the CC BY-NC-ND license (<http://creativecommons.org/licenses/by-nc-nd/4.0/>).

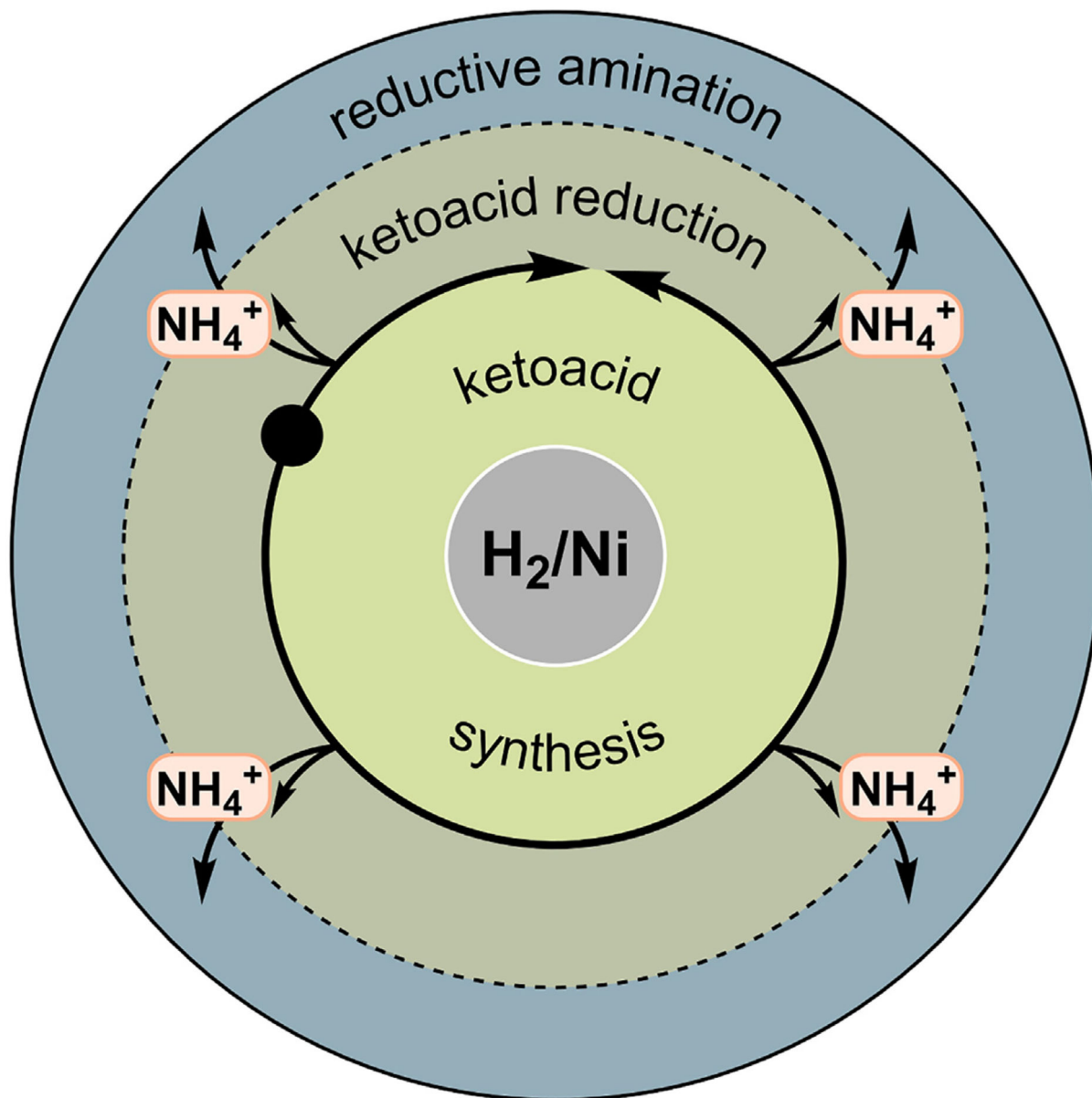
[†]Correspondence: moran@unistra.fr.

[‡]Lead contact

Declaration of Interests

The authors declare no competing interests.

Continuous Nonenzymatic Reaction Network



We show a metabolism-like continuous chemical reaction network driven by H_2 and catalyzed by nickel. Starting from glyoxylate and oxaloacetate, the nonenzymatic reaction network generates ketoacids by reductive aldol chemistry and converts them to hydroxy acids and amino acids. Six biological ketoacids and glyoxylate are converted to the corresponding amino acids using nickel or meteorites as catalysts. The results support the hypothesis that the earliest biochemical networks could have emerged without enzymes or RNA.

Introduction

Metabolic theories for the origin of life postulate that core microbial metabolism was pre-figured by naturally occurring reactions that became faster and more specific with the advent of enzymes.^{1–8} Dating at least as far back as the last universal common ancestor (LUCA), anabolic biochemistry was driven by H₂ gas produced by the Earth's crust^{9,10} and was built from CO₂, NH₃, H₂S, and phosphate, using reactions conserved in archaea and bacteria that use the acetyl CoA pathway for carbon and energy metabolism.^{11–13} In these anaerobic chemolithoautotrophs, carbon enters metabolism when H₂ reduces CO₂ to C1–C6 carboxylic acids and ketoacids via the acetyl CoA pathway and the incomplete reverse Krebs cycle,¹⁴ while nitrogen enters metabolism as ammonia via the reductive amination of α -ketoglutarate to glutamate (Figure 1A)¹⁵ and subsequent transaminations.¹⁶ In autotrophs using the acetyl CoA pathway, H₂ is the sole source of electrons for both carbon and nitrogen assimilation.

We and others have argued that a complex synthetic reaction network must have operated uninterrupted to support growth and evolutionary mechanisms, which, in turn, constrains the extent to which that reaction network could change.^{1–8} Consequently, metabolites supporting multiple pathways, key classes of chemical transformations, and energetic aspects of the primordial self-organized chemistry are expected to remain preserved in biological metabolism. In line with these predictions, several nonenzymatic reaction networks bearing similarities to metabolic pathways have been uncovered over the past 8 years, narrowing the gap between prebiotic chemistry and ancient microbial metabolism.^{5,17–19} However, although each of these pathways, or segments thereof, are continuous in isolation, chemical incompatibilities have thus far prevented their combination into larger continuous reaction networks. Experimental demonstrations of larger continuous prebiotic synthetic reaction network that are congruent with early biochemistry are thus critical to advancing our understanding of the origin of life.

Heterogeneous metal-catalyzed hydrogenation represents a textbook class of workhorse reactions in synthetic and industrial chemistry and has been used for the reduction of alkenes and ketones and for the reductive amination of ketones with ammonia, even in water.^{20–22} Hydrogen (H₂) is continuously produced by serpentinization in hydrothermal vents and hydrothermal fluids typically contain 1–15 mmol/kg of dissolved H₂.²³ Given the poor solubility of H₂ in water, these H₂ concentrations are not so different to hydrogenation reactions in synthetic organic chemistry carried out in water at H₂ pressures of <10 bar.²⁴ Given the robustness of metal-catalyzed hydrogenation, the high relevance of H₂ to metabolism and to ancient microbial ecosystems, and H₂'s geological relevance, it is perhaps surprising that until recently hydrogenation has rarely been exploited experimentally to understand the origin of metabolism. Analogs of core carbon fixation pathways have recently been demonstrated to be driven by H₂, using transition metals under mild conditions (22°C–25°C, near-neutral pH).^{25–27} In the case of the acetyl CoA pathway, the reaction of H₂ with CO₂ (25 bar, 2:3 ratio) to generate formate, acetate, and pyruvate occurred at 100°C²⁵ or at room temperature using the mineral awaruite (Ni₃Fe) as a catalyst.²⁶ For the reverse Krebs cycle, it was shown that Ni (10 mol%) supported on SiO₂-Al₂O₃, platinum group metals (1 mol%), or even ground meteorites could create the right conditions for H₂

(1–10 bar) to drive the sequence of reactions converting oxaloacetate to succinate at room temperature.²⁷ However, it remains unknown whether H₂ can enable the synthesis of more complex ketoacids and their reductive amination to amino acids under common conditions. Previous reports on prebiotic reductive amination have used stoichiometric iron species as the reducing agent,^{28–30} rather than H₂, and relied on relatively high³¹ concentrations of ammonia, ranging from 375 mM²⁸ to 1.5 M.²⁹ Alternatively, a stepwise reductive amination of ketoacids to amino acids has been reported using a Bucherer-Bergs reaction with cyanide and ammonia at 20°C, followed by decarboxylative hydrolysis of the resulting hydantoin at 80°C.³² However, in contrast to H₂, cyanide is never directly used in metabolism and is toxic to aerobic and anaerobic organisms due to its strong binding to a broad spectrum of metalloenzymes.³³ Even specialized organisms that have evolved to grow when cyanide is a limiting nutrient degrade it to CO₂ and ammonia before the latter can be assimilated³⁴; thus, its relevance to metabolic origins is questionable. Here, we report that using Ni/SiO₂-Al₂O₃ (10 mol% Ni) or platinum group metal catalysts (1 mol%), H₂ drives reductive amination of ketoacids using quantities of ammonia as low as 6 mM. We show that, under the same conditions, H₂ is able to drive the synthesis of higher ketoacids through reductive aldol reactions, analogous to the function of the reverse Krebs cycle, without consuming organic reducing agents.^{35,36} Finally, we demonstrate that these two H₂-driven processes can co-occur to produce a continuous reaction network that is strikingly similar to the core of ancient metabolism.

Results And Discussion

Reductive amination of pyruvate

To identify inorganic catalysts that could promote prebiotic reductive amination reactions, we performed catalyst screening for a wide spectrum of metals known for hydrogenation or reductive amination in synthetic chemistry.^{20,37} Homogeneous and heterogeneous forms of Earth-abundant metals found in biology were evaluated, such as Fe, Ni, and Co. Additionally, rarer platinum group metals, such as Ru, Rh, Pd, Ir, and Pt^{21,38} were also evaluated because trace elements not currently used as catalysts by biology may still potentially be relevant to initiate the origins of life.³⁹ We first assayed the reductive amination of pyruvate to alanine using mild conditions for the screening protocol: 5 equiv of NH₄⁺, 22°C, water at pH 7–8, and 5 bar of H₂ in the presence or absence of bicarbonate (supplementary excel file, Table S1). Alternatively, formate (5 equiv) was screened as a reducing agent. After 24 h, the yields were determined by quantitative ¹H NMR by integrating against dimethyl sulfone (DMS) as an internal standard (see Table S1 for the full screen). Under H₂ at pH 8, in the presence of bicarbonate, Ni/SiO₂-Al₂O₃ (10 mol% Ni, 320 ppm; hereafter referred to as Ni) and Pd/C (1 mol% Pd, 32 ppm; characterized as a mixture of Pd/C and PdO/C [Figures S72 and S73]; hereafter referred to as Pd) produced alanine in yields ranging from 18% to 40%, accompanied by the carbonyl reduction product lactate in 5%–15% yield and approximately 38 mM of formate derived from bicarbonate reduction⁴⁰ (15% yield based on the initial quantity of bicarbonate) (Figure 1B, entries 1 and 2). The latter result shows that reductive amination, carbonyl reduction, and bicarbonate reduction can occur concurrently in water. In the case of the Pd catalyst, reducing the pressure of H₂ to 1 bar instead of 5 bar gave similar yields but over longer reaction times (Table S1, entry

88). The observation of formate in the Pd-catalyzed experiment prompted us to investigate whether formate might also act as a reducing agent via transfer hydrogenation.⁴¹ This was found to be the case only for Pd, where formate (5 equiv) in the absence of H₂ yielded 53% alanine and 2% lactate (Figure 1B, entry 2). For the Ni catalyst, no reduction was observed in the absence of H₂, even in the presence of formate. No reduction occurred in the absence of metal catalysts (Table S1). For the reactions described above, the reaction pH of 7–8 resulted from the presence of bicarbonate or formate in 5-fold excess compared with the ketoacid. However, for either metal catalyst, when the reaction pH was manually adjusted, increased pH values generally favored amino acid formation whereas decreased pH values favored hydroxacid formation (Tables S3 and S4).

Lower ammonia concentrations

Previous reductive aminations involving metals in a prebiotic chemistry context^{28–30} have used ammonia in high concentrations³¹ and in vast excess compared with the ketoacid (100 equiv; 375 mM to 1.5 M ammonia). Although we used only 5 equiv of ammonia (150 mM) in our preliminary experiments, the high yields prompted us to test lower concentrations of ammonia. Indeed, when 6 mM of ammonia was used with 30 mM of pyruvate, alanine was obtained in up to 44% yield with Pd and up to 17% with Ni (yields relative to ammonia, Figure 1B, entries 3 and 4). This concentration of ammonia is 62 to 250 times lower than the previous reports. Although one might argue that the benefit of needing a lower ammonia concentration is offset by the need for an environment concentrated in a particular metal, we note that ammonia is a stoichiometric reagent whereas the metals are catalysts. Even though natural mechanisms exist for the generation^{42–44} and concentration⁴⁵ of ammonia, this concentration mechanism would need to operate continuously to enable the chemistry. In contrast, because the metal is a catalyst, its local concentration needs to only happen once to initiate the chemistry.

Meteorites as representative natural catalysts

These results suggested that simpler catalysts that are not man-made might also suffice. Because earthly geological samples from the time around life's origin no longer exist, and because modern geological samples may have been influenced by life, we elected to investigate iron meteorites as catalysts. Iron meteorites are representative of some of the objects that impacted Earth early in its history and are rich in Ni (up to 33%) and, in some cases, platinum group metals (Rh, Pt, and Pd in ppm amounts).^{46–53} The catalytic properties of iron meteorites in the context of prebiotic chemistry have been described before.^{54,55} It is not our intent here to invoke a prebiotic scenario involving meteorites but rather to investigate whether ancient heterogeneous geological samples, rather than man-made catalysts, can enable similar reactivity. Beyond meteorites, roughly 220 tonnes of metallic Fe-Ni arrives each year on the Earth in finely powdered form as cosmic dust.⁵⁶ Perhaps most importantly, tiny metallic Ni particles are found in hydrogen-rich hydrothermal vents.⁵⁷ Samples of ten representative iron meteorites whose compositions have already been studied in detail (11–18 mol% Ni; ppm amounts of Rh and Pd)^{46,52,53,58} were purchased and processed into a micro-powder for reproducibility and a larger surface area (Figure S74). Elemental analysis of representative particles of ground meteorite particles was performed by energy-dispersive X-ray spectroscopy (EDX) (Figure S75; Table S23). The samples were

tested as catalysts (3 mg) under the $\text{H}_2/\text{HCO}_3^-$ conditions described above. In all cases, amino and hydroxy acids were obtained. For example, the Aletai meteorite (18 mol% Ni)⁵⁸ gave alanine in 24% yield and lactate in 43% yield (Figure 1B, entry 5; for other meteorites, see Table S1). Importantly, control experiments without H_2 did not produce any reaction products, demonstrating that the meteoritic metals do not act as reductants (Table S1).

Reductive amination of glyoxylate and α -ketoacids

To test the substrate specificity of the reactions, we explored reductive amination of glyoxylate and the α -ketoacids that generate amino acids in metabolism. Under our standard conditions, the Ni, Pd, and Aletai meteorite catalysts were found to be compatible with glyoxylate and six different biological α -ketoacids (pyruvate, α -ke-toglutarate, oxaloacetate, α -ketoisocaproate, α -ketoisovalerate, and α -keto- β -methylvalerate) to give a mixture of the corresponding amino acids (glycine, alanine, glutamate, aspartate, leucine, valine, and isoleucine) and hydroxyacids (Figure 2). In the case of the Ni and meteorite catalysts, the product mixture was obtained in 6%–84% yield in a roughly equal ratio of amino- and hydroxyacids. In the case of the Pd catalyst, the product mixture was obtained in 52%–88% yield with >5:1 selectivity favoring the α -amino acid over the α -hydroxy acid in almost all cases. When formate (5 equiv) was used as a reducing agent instead of $\text{H}_2/\text{HCO}_3^-$, the Pd catalyst delivered the amino acids with similar yields and selectivity (Table S9; Figures S43–S48). In the absence of the catalyst, no reduction products were observed (Tables S8 and S10; Figures S36–S42 and S49–S54).

Reductive aldol chemistry of ketoacids under H_2

Having found a general H_2 -driven reductive amination of α -ketoacids under potential prebiotic conditions, we asked whether α -ketoacids can be simultaneously generated and converted to amino acids as in metabolism, but using these catalysts rather than enzymes. Recently, Fe^{2+} or phosphate was shown to catalyze reductive aldol chemistry, derived from the reaction of pyruvate or oxaloacetate with glyoxylate to form a series of α -ketoacids, including α -ketoglutarate, in functional analogy to the reverse Krebs cycle.^{35,36} The chemistry involves an initial aldol reaction to form maloyl formate and dehydration to form fumaroyl formate. The reduction of the alkene moiety of fumaroyl formate, using glyoxylate hydrate as the reducing agent, yields α -ketoglutarate, which then undergoes a second aldol reaction generating isocitroyl formate, followed by dehydration to give aconitoyl formate (Figure 3, circle 2 [rTCA cycle homolog]).

Although the aldol condensation chemistry is easy and proceeds even without catalysis at 22°C, the reduction of fumaroyl formate using glyoxylate requires higher temperatures (50°C–70°C) and an excess of Fe^{2+} (200 mol%) or phosphate (500 mol%).^{35,36} We tested whether H_2 rather than glyoxylate hydrate might also drive the key reduction step under the same conditions discovered for reductive amination, allowing the two processes to operate simultaneously. First, we aimed to establish whether the reductive aldol chemistry could be driven by H_2 in the absence of ammonia. Indeed, simply mixing oxaloacetate and glyoxylate under the standard Ni- or Pd-catalyzed conditions (22°C, water at pH 7–8 and 5 bar of H_2 in the presence or absence of bicarbonate, 72 h) allowed us to detect and quantify all the expected products of the reductive aldol chemistry shown in Figure

3, circle 2 (maloyl formate, fumaroyl formate, α -ketoglutarate, isocitroyl formate, and aconitoyl formate); pyruvate derived from spontaneous decarboxylation of oxaloacetate; and hydroxyacids derived from carbonyl reduction of the α -ketoacid starting materials and intermediates (glycolate and lactate). ^1H NMR of a representative crude reaction mixture for the Ni-catalyzed process reveals the spectrum shown in Figure 4A. Assuming the reaction network stoichiometries described in Figure 3, the 9 compounds derived from oxaloacetate accounted for ~62% total yield with respect to the oxaloacetate employed, with one further product derived only from glyoxylate (glycolate) comprising an additional 23% yield with respect to glyoxylate. Using the Pd catalyst, the same products accumulated using either $\text{H}_2/\text{HCO}_3^-$ or formate (Tables S12 and S15; Figures S58 and S63); malate could additionally be observed with Pd. In the absence of catalyst, the initial products of aldol condensation, maloyl formate, and fumaroyl formate, were still observed but not the products downstream of the reduction of fumaroyl formate (Tables S17–S20; Figures S66–S69). The reaction network was not studied at higher temperatures because oxaloacetate decarboxylates to pyruvate under such conditions.

Combining reductive aldol chemistry and reductive amination

With common H_2 - or formate-driven conditions in hand for reductive amination and for the α -ketoacid-generating reductive aldol reactions, we explored the possibility of linking these processes into a continuous reaction network in a single environment—as it occurs in real metabolism. Previous work has indicated that they are mutually incompatible. For example, metallic Fe and hydroxylamine convert ketoacids to amino acids but disrupt Fe^{2+} -promoted ketoacid formation via reductive aldol chemistry.³⁵ Likewise, Al^{3+} -catalyzed transamination converts ketoacids to amino acids but could not be carried out in the presence of phosphate-mediated reductive aldol chemistry.³⁶ However, simply mixing oxaloacetate and glyoxylate under the standard Ni- or Pd-catalyzed conditions, but in the presence of ammonium bicarbonate (22°C, water at pH 7–8 and 5 bar of H_2 , 72 h), allowed us to detect all the expected products of the reductive aldol chemistry (maloyl formate, fumaroyl formate, α -ketoglutarate, isocitroyl formate, and aconitoyl formate); pyruvate derived from spontaneous decarboxylation of oxaloacetate; hydroxyacids derived from carbonyl reduction of the α -ketoacid starting materials and intermediates (glycolate, lactate, and malate), as well as three amino acids (glycine, aspartate, and alanine). The amino acids formed in the one-pot experiment notably include glycine and aspartate, whose carbon frameworks become incorporated into purines and pyrimidines, respectively, during biosynthesis.

A ^1H NMR of a representative crude reaction mixture in the presence of Ni catalyst is shown in Figure 4B, accounting for ~37% total yields of products. Reaction yields of all products were determined by quantitative ^1H NMR integrating against dimethyl sulfone as an internal standard at pH 8, with the exception of aspartate, which was detected by gas chromatography-mass spectrometry (GC-MS) (Table S14; Figures S61 and S62, supporting information). The Pd catalyst, using $\text{H}_2/\text{HCO}_3^-$ or formate as a reducing agent, generated the same products in a comparable combined yield, with a slightly different distribution across the various compounds (Tables S11 and S13; Figures S55–S57, S59, and S60). In this case, aspartate was detected in roughly 5% yield by ^1H NMR. Compared with the experiments carried out in the absence of ammonia, its presence gave rise to several side

reactions, particularly in the case of Ni catalysis. Products beyond those described in Figure 3 could be observed by NMR or GC-MS analysis but could not be identified. Compared with the Pd catalyst, the Ni catalyst furnished a wider range of products of biological interest, including glutamate, hydroxyketoglutarate, and alanine. Similar reactivity was observed when the experiments were scaled up 10-fold, although the initial decarboxylative aldol reaction was slower in this case (Tables S21 and S22; Figures S70 and S71).

Conclusions

In summary, we have shown that H₂ in the presence of suitable metal catalysts under simple, aqueous, low ammonia conditions can drive amino acid synthesis via reductive amination of ketoacids under the same conditions needed for complex ketoacid synthesis via hydrogenative aldol chemistry and carbonyl reduction. Working together in a single pot without further intervention from the experimenter, the resulting reaction network emulates interconnected biosynthetic pathways at the heart of microbial metabolism, relying on H₂^{59,60} or formate^{61,62} to drive reductive reactions and on ammonium as a nitrogen source. The keys to this hydrogenation chemistry are heterogeneous metal catalysts based on Ni (10 mol%) or Pd (1 mol%). Either metal supplies the catalytic function of over a dozen enzymes and their associated cofactors at the core of microbial metabolism. The reactions occur at ambient temperature, at near-neutral pH, and with H₂ as the reductant under mild aqueous conditions relevant to geochemical H₂ synthesis in hydrothermal systems⁹ and metabolic origin.¹³

The observation that meteorite samples catalyze amino acid synthesis substantially strengthens the case for natural minerals being able to promote reactions central to microbial metabolism.^{3–5,9,25} The meteorite samples shown to be active were 11–18 mol% Ni, whereby their heterogeneous composition does not allow us to attribute this reactivity to a particular metal, or mixture of metals, or to exclude a role for trace metals. Ni is common in meteorites,⁶³ in H₂-producing hydrothermal vents,^{25,64} and in the active site of enzymes involved in the acetyl CoA pathway,⁶⁵ whereas platinum group metals like Pd are rare in the environment and lacking in enzymes altogether. In our attempts to combine ketoacid generation with reductive amination, Ni also furnished a wider spectrum of biologically relevant products than did Pd. Although Ni has more appeal in these regards, it may be premature to entirely dismiss platinum group metals as prebiotic catalysts because they are active even at ppm levels and are, in nature, locally concentrated in amounts many orders of magnitude higher than their average abundance in the Earth's crust.²⁷ For example, Pd has been found in certain samples of pentlandite in concentrations of up to 11 wt.%.⁶⁶ In this work, we found no reactions that were specifically dependent upon Pd, as they could all be catalyzed by Ni, though sometimes in lower yields. The Ni-catalyzed conditions identified in this study are relevant to environments with high natural concentrations of H₂, including hydrothermal vents that generate H₂ through serpentinization and underground caverns that collect and concentrate H₂ produced by water radiolysis deeper in the Earth's crust. Each of these processes is thought to have generated 10¹¹ mol of H₂ per year during the pre-Cambrian era.⁶⁷ Importantly, H₂ is not released uniformly throughout the planet but is focused through specific environments like hydrothermal vents, where H₂-breathing organisms still live today. Complementing Ni catalysis, the Pd-catalyzed

conditions identified in this study can either rely on H₂ or enable transfer hydrogenation from formate. Taken together, these two metals offer a complementary range of conditions where hydrogenation or transfer hydrogenation might become prebiotically relevant. Various sources of energy and catalysis have been proposed as the driver of early chemical evolution. The reactions reported here generate ketoacids of the rTCA cycle and seven biological amino acids in correspondence to the reactions comprising central microbial metabolism with no need for peptides, RNA, cofactors, metal sulfides,⁶⁸ organosulfides,⁶⁹ cyanides,⁷⁰ or ultraviolet light.⁷¹ This study supports the idea that the core of microbial metabolism, fed by pyruvate synthesis,^{25,26} could have arisen from metal-catalyzed reactions of CO₂, H₂O, and NH₃, fueled by geochemical H₂ (or formate) in darkness.

Experimental Procedures

Resource availability

Lead contact—Requests for further information and resources should be directed to and will be fulfilled by the lead contact, Joseph Moran (moran@unistra.fr).

Materials availability—All materials generated in this study are available from the lead contact.

Supplementary Material

Refer to Web version on PubMed Central for supplementary material.

Acknowledgments

This project has received funding from the European Research Council (ERC) under the European Union's Horizon 2020 research and innovation programme (grant agreements nos. 101001752 and 101018894 and Marie Skłodowska Curie grant agreement no. 813873). The work was also supported by the Interdisciplinary The-matic Institute ITI-CSC via the IdEx Unistra (ANR-10-IDEX-0002) within the program Investissement d'avenir. J.M., H.T., and W.F.M. thank the VW Foundation (no. 96_742) for generous support. E.W. thanks the ENS for a PhD fellowship. H.T. thanks FUNCAT and the Max Planck Society for the basic funding. We thank Dr. Robert Mayer, Dr. Kamila Muchowska, and Dr. Martina Preiner for discussions.

Data and code availability

All data supporting this study are available in the manuscript or supplementary information.

All data are available in the supplementary information file (supplemental experimental procedures; Figures S1–S75; Tables S2–S23). Table S1 reporting the metal catalyst screening for reductive amination of pyruvate to alanine under different reaction conditions (H₂, H₂/HCO₃[−], or HCO₂[−]) can be found as an attached supplementary excel file.

References

1. Martin WF. Older than genes: The acetyl CoA pathway and origins. *Front Microbiol.* 2020; 11: 817. [PubMed: 32655499]
2. Stockbridge RB, Lewis CA, Yuan Y, Wolfenden R. Impact of temperature on the time required for the establishment of primordial biochemistry, and for the evolution of enzymes. *Proc Natl Acad Sci USA.* 2010; 107: 22102–22105. [PubMed: 21123742]

3. Martin W, Russell MJ. On the origin of biochemistry at an alkaline hydrothermal vent. *Trans Roy Società B.* 2007; 362: 1887–1925.
4. Smith, E, Morowitz, HJ. The origin and nature of life on earth: the emergence of the fourth geosphere. Cambridge University Press; New York, NY: 2016.
5. Muchowska KB, Varma SJ, Moran J. Nonenzymatic metabolic reactions and Life's origins. *Chem Rev.* 2020; 120: 7708–7744. [PubMed: 32687326]
6. Ralser M, Varma SJ, Notebaart RA. The evolution of the metabolic network over long timelines. *Curr Opin Syst Biol.* 2021; 28 100402
7. Noda-Garcia L, Liebermeister W, Tawfik DS. Metabolite–enzyme coevolution: from single enzymes to metabolic pathways and networks. *Annu Rev Biochem.* 2018; 87: 187–216. [PubMed: 29925259]
8. Harrison SA, Lane N. Life as a guide to prebiotic nucleotide synthesis. *Nat Commun.* 2018; 9 5176 [PubMed: 30538225]
9. Preiner M, Xavier JC, Sousa FL, Zimorski V, Neubeck A, Lang SQ, Greenwell HC, Kleinerkmann K, Tüysüz H, McCollom TM, et al. Serpentinization: connecting geochemistry, ancient metabolism and industrial hydrogenation. *Life (Basel).* 2018; 8: 41. [PubMed: 30249016]
10. Sherwood Lollar BS, Heuer VB, McDermott J, Tille S, Warr O, Moran JJ, Telling J, Hinrichs K-U. A window into the abiotic carbon cycle – Acetate and formate in fracture waters in 2.7-billion-year-old host rocks of the Canadian Shield. *Geochim Cosmochim Acta.* 2021; 294: 295–314.
11. Wimmer JLE, Xavier JC, Vieira ADN, Pereira DPH, Leidner J, Sousa FL, Kleinerkmann K, Preiner M, Martin WF. Energy at origins: Favorable thermodynamics of biosynthetic reactions in the last universal common ancestor (LUCA). *Front Microbiol.* 2021; 12 793664 [PubMed: 34966373]
12. Weiss MC, Sousa FL, Mrnjavac N, Neukirchen S, Roettger M, Nelson-Sathi S, Martin WF. The physiology and habitat of the last universal common ancestor. *Nat Microbiol.* 2016; 1 16116 [PubMed: 27562259]
13. Fuchs G. Alternative pathways of carbon dioxide fixation: Insights into the early evolution of life? *Annu Rev Microbiol.* 2011; 65: 631–658. [PubMed: 21740227]
14. Fuchs, G, Stupperich, E. Evolution of Prokaryotes. Schleifer, KH, Stackebrandt, E, editors. Academic Press; 1985. 235–251.
15. McMurry, JE, Begley, TP. The Organic Chemistry of Biological Pathways. Second Edition. Roberts and Company; 2016.
16. Mayer RJ, Kaur H, Rauscher SA, Moran J. Mechanistic insight into metal ion-catalyzed transamination. *J Am Chem Soc.* 2021; 143: 19099–19111. [PubMed: 34730975]
17. Yi J, Kaur H, Kazöne W, Rauscher SA, Gravillier LA, Muchowska KB, Moran J. A Nonenzymatic Analog of Pyrimidine Nucleobase Biosynthesis. *Angew Chem Int Ed Engl.* 2022; 61 e202117211 doi: 10.1002/anie.202117211 [PubMed: 35304939]
18. Dherbassy Q, Mayer RJ, Muchowska KB, Moran J. Metal-Pyridoxal Cooperativity in Nonenzymatic Transamination. *J Am Chem Soc.* 2023; 145: 13357–13370. DOI: 10.1021/jacs.3c03542 [PubMed: 37278531]
19. Werner E, Pinna S, Mayer RJ, Moran J. Metal/ADP complexes promote phosphorylation of ribonucleotides. *J Am Chem Soc.* 2023; 145: 21630–21637. [PubMed: 37750669]
20. Wu, X, Xiao, J. Metal-Catalyzed Reactions in Water. Dixneuf, P, Cadierno, V, editors. Wiley-VCH Verlag GmbH & Co. KGaA; 2013.
21. Knoop F, Oesterlin H. Über die natürliche Synthese der Aminosäuren und ihre experimentelle Reproduktion. *Hoppe Seylers Z Physiol Chem.* 1925; 148: 294–315.
22. Nakamura S, Ashida K. Studies on the Formation of Amino Acids from Keto Acids. *Nippon No-geikagaku Kaishi.* 1950; 24: 185–187.
23. Ueda H, Shibuya T, Sawaki Y, Shozugawa K, Makabe A, Takai K. Chemical nature of hydrothermal fluids generated by serpentinization and carbonation of komatiite: Implications for H₂-rich hydrothermal system and ocean chemistry in the early Earth. *Geochem Geophys Geosyst.* 2021; 22 GC009827.e2021
24. Kolev, NI. Multiphase Flow Dynamics, 4 Turbulence, Gas Absorption and release, diesel fuel properties. Second Edition. Springer; 2012.

25. Preiner M, Igarashi K, Muchowska KB, Yu M, Varma SJ, Kleinermanns K, Nobu MK, Kamagata Y, Tüysüz H, Moran J, et al. A hydrogen-dependent geochemical analogue of primordial carbon and energy metabolism. *Nat Ecol Evol.* 2020; 4: 534–542. [PubMed: 32123322]
26. Beyazay T, Belthle KS, Farès C, Preiner M, Moran J, Martin WF, Tüysüz H. Ambient temperature conversion of CO₂ and H₂ to pyruvate and citramalate over iron and nickel nanoparticles. *Nat Commun.* 2023; 14: 570. [PubMed: 36732515]
27. Rauscher SA, Moran J. Hydrogen drives part of the reverse Krebs cycle under metal or meteorite catalysis. *Angew Chem Int Ed Engl.* 2022; 61 e202212932 [PubMed: 36251920]
28. Barge LM, Flores E, Baum MM, VanderVelde DG, Russell MJ. Redox and pH gradients drive amino acid synthesis in iron oxyhydroxide mineral systems. *Proc Natl Acad Sci USA.* 2019; 116: 4828–4833. [PubMed: 30804197]
29. Huber C, Wächtershäuser G. Primordial reductive amination revisited. *Tetrahedron Lett.* 2003; 44: 1695–1697.
30. Kitadai N, Nakamura R, Yamamoto M, Takai K, Yoshida N, Oono Y. Metals likely promoted protometabolism in early ocean alkaline hydrothermal systems. *Sci Adv.* 2019; 5 eaav7848 [PubMed: 31223650]
31. Bada JL, Miller SL. Ammonium ion concentration in the Primitive Ocean. *Science.* 1968; 159: 423–425. [PubMed: 5634660]
32. Yadav M, Pulletikurti S, Yerabolu JR, Krishnamurthy R. Cyanide as a primordial reductant enables a protometabolic reductive glyoxylate pathway. *Nat Chem.* 2022; 14: 170–178. [PubMed: 35115655]
33. Rossifanelli A, Antonini E, Caputo A. Hemoglobin and myoglobin. *Adv Protein Chem.* 1964; 19: 73–222. [PubMed: 14268787]
34. Luque-Almagro VM, Cabello P, Sáez LP, Olaya-Abril A, Moreno-Vivián C, Roldán MD. Exploring anaerobic environments for cyanide and cyano-derivatives microbial degradation. *Appl Microbiol Biotechnol.* 2018; 102: 1067–1074. [PubMed: 29209795]
35. Muchowska KB, Varma SJ, Moran J. Synthesis and breakdown of universal metabolic precursors promoted by iron. *Nature.* 2019; 569: 104–107. [PubMed: 31043728]
36. Stubbs RT, Yadav M, Krishnamurthy R, Springsteen G. A plausible metal-free ancestral analogue of the Krebs cycle composed entirely of α -ketoacids. *Nat Chem.* 2020; 12: 1016–1022. [PubMed: 33046840]
37. Irrgang T, Kempe R. Transition-metal-catalyzed reductive amination employing hydrogen. *Chem Rev.* 2020; 120: 9583–9674. [PubMed: 32812752]
38. Ogo S, Uehara K, Abura T, Fukuzumi S. pH-dependent chemoselective synthesis of α -amino acids. reductive amination of α -keto acids with ammonia catalyzed by acid-stable iridium hydride complexes in water. *J Am Chem Soc.* 2004; 126: 3020–3021. [PubMed: 15012110]
39. Hazen RM, Morrison SM. Prebiotic Chemistry and the Origin of Life. *Adv Astrobiol Biogeop.* 2021. 43–61.
40. Stalder CJ, Chao S, Summers DP, Wrighton MS. Supported Palladium catalysts for the reduction of sodium bicarbonate to sodium formate in aqueous solution at room temperature and one atmosphere of hydrogen. *J Am Chem Soc.* 1983; 105: 6318–6320.
41. Zoran A, Sasson Y, Blum J. Catalytic transfer hydrogenation of unsaturated compounds by solid sodium formate in the presence of palladium on carbon. *J Mol Catal.* 1984; 26: 321–326.
42. Dörr M, Kässbohrer J, Grunert R, Kreisel G, Brand WA, Werner RA, Geilmann H, Apfel C, Robl C, Weigand W. A possible prebiotic formation of ammonia from dinitrogen on iron sulfide surfaces. *Angew Chem Int Ed Engl.* 2003; 42: 1540–1543. [PubMed: 12698495]
43. Grosch M, Stiebritz MT, Bolney R, Winkler M, Jückstock E, Busch H, Peters S, Siegle AF, van Slageren J, Ribbe M, et al. Mackinawite-supported reduction of c1 substrates into prebiotically relevant precursors. *ChemSystemsChem ChemSystemsChem.* 2022; 4 e202200010
44. Shang X, Huang R, Sun W. Formation of ammonia through serpentinization in the Hadean Eon. *Sci Bull (Beijing).* 2023; 68: 1109–1112. [PubMed: 37179231]
45. Takahagi W, Okada S, Matsui Y, Ono S, Takai K, Takahashi Y, Kitadai N. Extreme accumulation of ammonia on electroreduced mackinawite: An abiotic ammonia storage mechanism in early

- ocean hydrothermal systems. *Proc Natl Acad Sci USA*. 2023; 120 e2303302120 [PubMed: 37782799]
46. Ryan DE, Holzbecher J, Brooks RR. Rhodium and osmium in iron meteorites. *Chem Geol*. 1990; 85: 295–303.
 47. Gopakumar A, Akçok I, Lombardo L, Le Formal F, Magrez A, Sivula K, J Dyson P. Iron-rich natural mineral Gibeon meteorite catalyzed n-formylation of amines using CO₂ as the C1 source. *ChemistrySelect*. 2018; 3: 10271–10276.
 48. Le Formal F, Guijarro N, Boureé WS, Gopakumar A, Prévot MS, Daubry A, Lombardo L, Sornay C, Voit J, Magrez A, et al. A gibeon meteorite yields a high-performance water oxidation electrocatalyst. *Energy Environ Sci*. 2016; 9: 3448–3455.
 49. Bizzarri BM, Fanelli A, Kapralov M, Krasavin E, Saladino R. Meteorite-catalyzed intermolecular trans-glycosylation produces nucleosides under proton beam irradiation. *RSC Adv*. 2021; 11: 19258–19264. [PubMed: 35478633]
 50. Saladino R, Botta L, Di Mauro E. The prevailing catalytic role of meteorites in formamide prebiotic processes. *Life (Basel)*. 2018; 8: 6. [PubMed: 29470412]
 51. Cabedo V, Llorca J, Trigo-Rodríguez JM, Rimola A. Study of fischer–tropsh-type reactions on chondritic meteorites. *Astron Astro Phys*. 2021; 650 A160
 52. Scott ERD. *Handbook of Iron Meteorites*. Meteorit Planet Sci. 1975; 48 2608
 53. Krot, AN, , et al. *Treatise on Geochemistry*. Second Edition. Turekian, KK, editor. Elsevier; HD Holland: 2014. 1–63.
 54. Bizzarri BM, Fanelli A, Kapralov M, Krasavin E, Saladino R. Meteorite-catalyzed intermolecular trans-glycosylation produces nucleosides under proton beam irradiation. *RSC Adv*. 2021; 11: 19258–19264. [PubMed: 35478633]
 55. Peters S, Semenov DA, Hochleitner R, Trapp O. Synthesis of prebiotic organics from CO₂ by catalysis with meteoritic and volcanic particles. *Sci Rep*. 2023; 13 6843 [PubMed: 37231067]
 56. Bones DL, Carrillo-Sánchez JD, Kulak AN, Plane JMC. Ablation of Ni from micrometeoroids in the upper atmosphere: Experimental and computer simulations and implications for Fe ablation. *Planet Space Sci*. 2019; 179 104725
 57. Dekov V. Native nickel in the TAG hydrothermal field sediments (mid-Atlantic Ridge, 26°N): Space trotter, guest from mantle, or a widespread mineral, connected with serpentinization? *J Geophys Res*. 2006; 111
 58. Xu L, Miao B, Lin Y, Ouyang Z. Ulasitai: A new iron meteorite likely paired with armanty (IIIIE). *Meteorit & Planetary Sci*. 2008; 43: 1263–1273.
 59. Thauer RK, Kaster AK, Seedorf H, Buckel W, Hedderich R. Methanogenic archaea: Ecologically relevant differences in energy conservation. *Nat Rev Microbiol*. 2008; 6: 579–591. [PubMed: 18587410]
 60. Müller V, Chowdhury NP, Basen M. Electron bifurcation: A long-hidden energy-coupling mechanism. *Annu Rev Microbiol*. 2018; 72: 331–353. [PubMed: 29924687]
 61. Lang SQ, Früh-Green GL, Bernasconi SM, Brazelton WJ, Schrenk MO, McGonigle JM. Deeply-sourced formate fuels sulfate reducers but not methanogens at Lost City hydrothermal field. *Sci Rep*. 2018; 8: 755. [PubMed: 29335466]
 62. Colman DR, Kraus EA, Thieringer PH, Rempfert K, Templeton AS, Spear JR, Boyd ES. Deep-branching acetogens in serpentinized subsurface fluids of Oman. *Proc Natl Acad Sci USA*. 2022; 119 e2206845119 [PubMed: 36215489]
 63. Bonal L, Gattacceca J, Garenne A, Eschrig J, Rochette P, Krämer Ruggiu L. Water and heat: New constraints on the evolution of the CV chondrite parent body. *Geochim Cosmochim Acta*. 2020; 276: 363–383.
 64. Ellison ET, Templeton AS, Zeigler SD, Mayhew LE, Kelemen PB, Matter JM. Low-temperature hydrogen formation during aqueous alteration of serpentinized peridotite in the Samail ophiolite. *J Geophys Res Solid Earth*. 2021; 126 JB021981.e2021
 65. Ragsdale SW. Nickel-based enzyme systems. *J Biol Chem*. 2009; 284: 18571–18575. [PubMed: 19363030]

66. Kalugin V, Gusev V, Tolstykh N, Lavrenchuk A, Nigmatulina E. Origin of the Pd-Rich Pentlandite in the Massive Sulfide Ores of the Talnakh Deposit, Norilsk Region, Russia. *Minerals*. 2021; 11: 1258
67. Lollar BS, Onstott TC, Lacrampe-Couloume G, Ballentine CJ. The contribution of the Precambrian continental lithosphere to global H₂ production. *Nature*. 2014; 516: 379–382. [PubMed: 25519136]
68. Wächtershäuser G. Groundworks for an evolutionary biochemistry – the iron sulfur world. *Prog Biophys Mol Biol*. 1992; 58: 85–201. [PubMed: 1509092]
69. Goldford JE, Hartman H, Marsland R, Segrè D. Environmental boundary conditions for the origin of life converge to an organo-sulfur metabolism. *Nat Ecol Evol*. 2019; 3: 1715–1724. [PubMed: 31712697]
70. Orgel LE. Prebiotic chemistry and the origin of the RNA world. *Crit Rev Biochem Mol Biol*. 2004; 39: 99–123. [PubMed: 15217990]
71. Patel BH, Percivalle C, Ritson DJ, Duffy CD, Sutherland JD. Common origins of RNA, protein and lipid precursors in a cyanosulfidic protometabolism. *Nat Chem*. 2015; 7: 301–307. [PubMed: 25803468]

Highlights

Continuous H₂-driven abiotic metabolism-like reaction network

Ketoacid-forming reductive aldol chemistry co-occurring with reductive amination

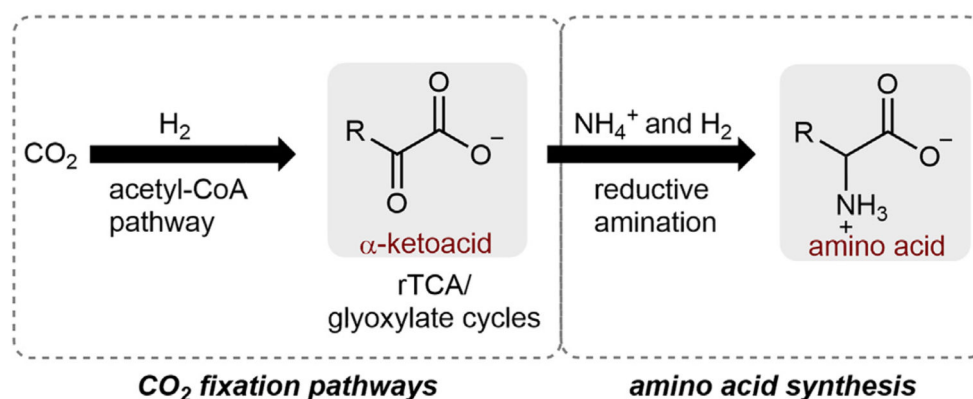
Mild conditions (pH 8, 22°C) with catalytic amounts of nickel or ground meteorites

Low ammonium concentrations 6–150 mM

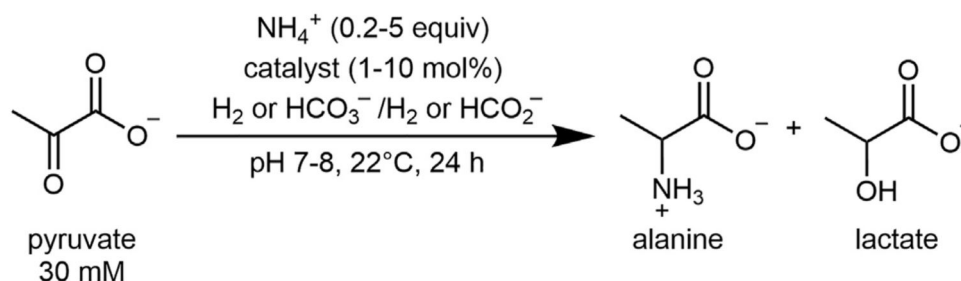
The Bigger Picture

The “metabolism-first” hypothesis for the origin of life suggests that life grew out of a geochemical reaction network that resembled the core of microbial metabolism. Recent experiments show that subsets of such a network could be recreated without enzymes, but they operate under distinct conditions and are rarely powered by the reducing agents used by biology, such as hydrogen gas. A major challenge is to identify conditions where multiple metabolic subnetworks can work together as a coherent whole. We report that nickel catalysts allow hydrogen gas to drive reactions analogous to amino acid biosynthesis and the reverse Krebs cycle under common mild conditions. The reactions collectively resemble the core of microbial metabolism and occur together in one pot without human intervention.

A General scheme from CO₂ fixation pathways to amino acid synthesis



B Reductive amination of pyruvate to alanine under H₂ with metal catalysts and meteorite



Entry	Catalyst	[NH ₄] ⁺ (mM)	Yield (%) ^[f]				
			H ₂ /HCO ₃ ⁻ (5 bar/5 equiv, pH 8) ^[a]			HCO ₂ ⁻ (5 equiv, pH 7) ^[b]	
			alanine	lactate	formate ^[e]	alanine	lactate
1 ^[g]	Ni/SiO ₂ -Al ₂ O ₃ (10 mol%)	150	17.5 ± 0.6	15.2 ± 0.1	n. d.	n. d.	n. d.
2 ^[g]	Pd/C (1 mol%)	150	39.7 ± 5.0	4.9 ± 0.7	~ 14.6 ± 1.4	52.5 ± 0.2	1.7 ± 0.1
3	Ni/SiO ₂ -Al ₂ O ₃ (10 mol%)	6 ^[d]	16.7	53.1	n. d.	n. d.	n. d.
4	Pd/C (1 mol%)	6 ^[d]	20.5	47.0	~ 15	44.3	8
5	Aletai meteorite (3 mg) ^[c]	150	24 ± 2	43 ± 1	n. d.	n. d.	n. d.

Figure 1. Amino acid synthesis

(A) Core biological carbon fixation pathways and amino acid biosynthesis driven by H₂.

(B) Reductive amination of pyruvate to alanine: pyruvate (30 mM), catalyst, ammonium, and hydrogen source, 1 mL H₂O (pH 7–8), 22°C, 24 h. ^[a]Reaction with ammonium bicarbonate (NH₄HCO₃, 5 equiv, 150 mM, entries 1, 2, and 5) and (NH₄HCO₃, 0.2 equiv, 6 mM and NaHCO₃, 0.8 equiv, 144 mM, entries 3 and 4) under H₂ pressure (5 bar); ^[b]Reaction with ammonium formate (NH₄HCO₂, 5 equiv, 150 mM, entries 1, 2, and 5) and (NH₄HCO₂, 0.2 equiv, 6 mM and NaHCO₂ 0.8 equiv, 144 mM, entries 3 and 4) where formate is used as a hydride and CO₂ source; ^[c]Aletai meteorite composition for 3 mg ground powder: Ni (18 mol%), Co (0.01 mol%), Ir, Rh (ppb amounts), and Fe; ^[d]Alanine yields were calculated with respect to 6 mM of ammonia, while lactate yields were calculated with respect to

30 mM of pyruvate. ^[e]Formate yields were calculated with non-quantitative method with respect to 150 mM of bicarbonate; ^[f]Yields and average deviations (when duplicates) were determined by quantitative ¹H NMR spectroscopy with dimethyl sulfone as an internal standard. n.d., not detected; ^[g]N = 2. For details see Figures S1–S10 and Tables S1 and S2.

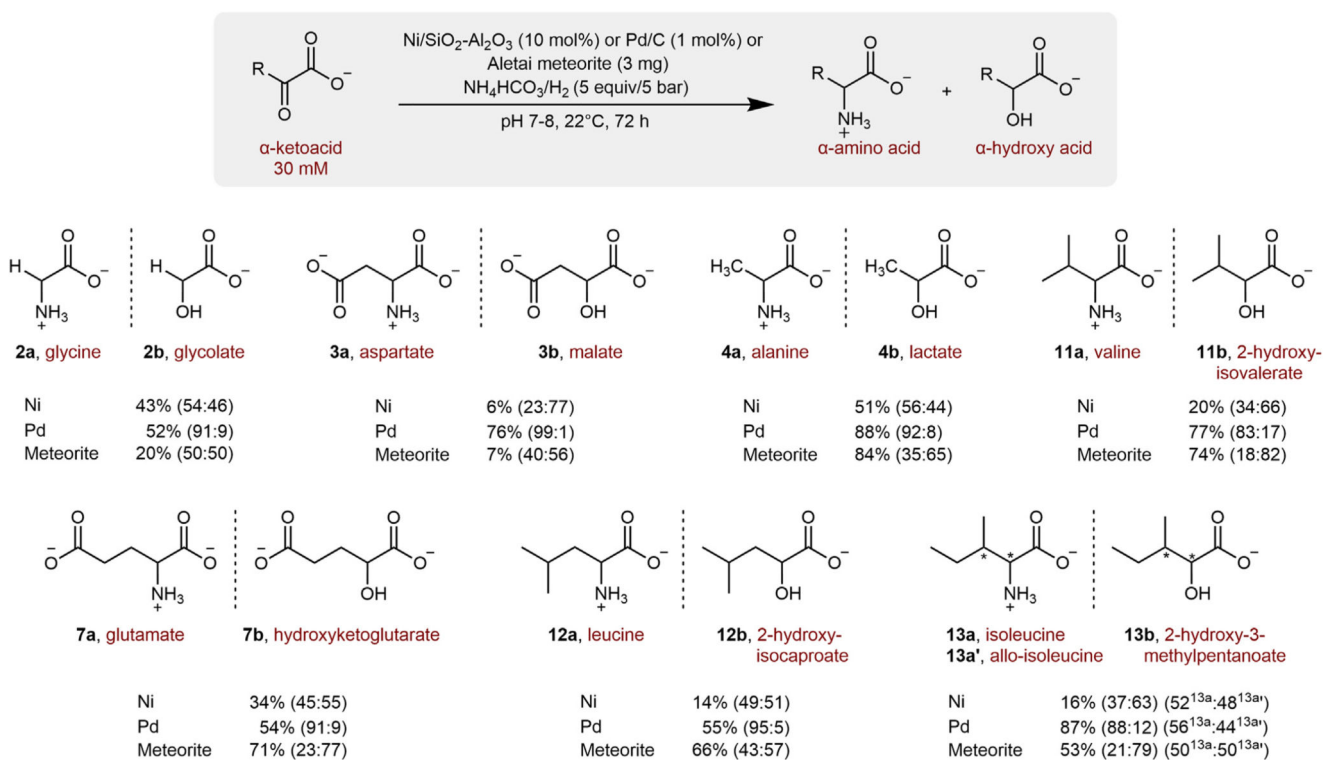


Figure 2. Nonenzymatic reductive amination generates biological amino acids under mild conditions

α -ketoacids (0.03 M) are converted to a mixture of α -amino acids and α -hydroxy acids upon exposure to $\text{H}_2/\text{NH}_4\text{HCO}_3$ (5 bars/5 equiv) under catalysis from Pd/C (1 mol% Pd, 32 ppm relative to substrate), Ni/SiO₂-Al₂O₃ (10 mol% Ni, 320 ppm relative to substrate), and Aletai meteorite (3 mg, 18 mol% Ni, 576 ppm relative to substrate) in pH 8 water at 22°C for 72 h. Percent yields refer to the combined yields of both products, with the amino acid/hydroxy acid product ratios given in parentheses. For details see Figures S11–S31 and Tables S5–S7.

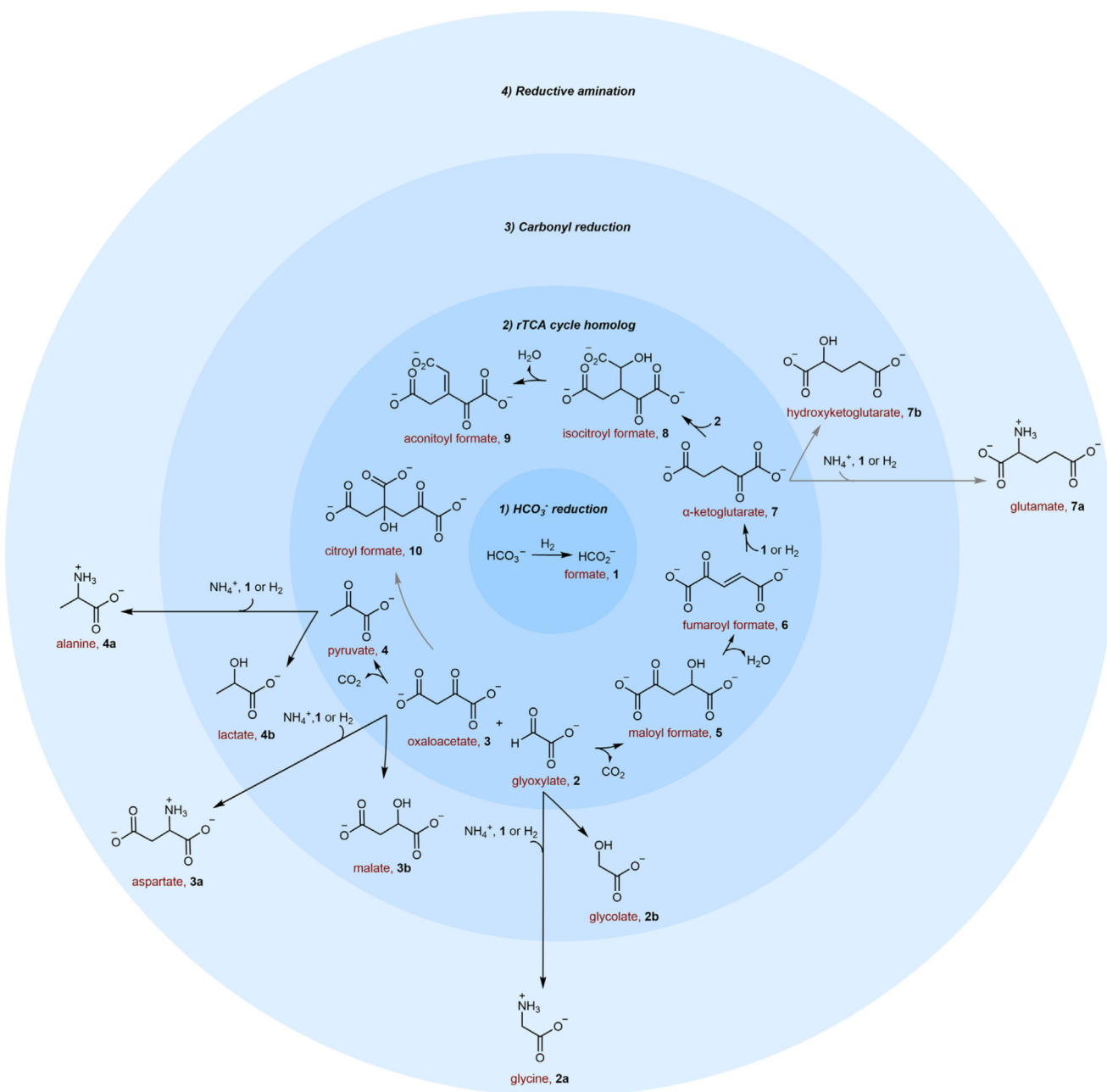


Figure 3. A nonenzymatic H_2 -driven reaction network spanning four different metabolism-like subsystems

The reaction network generated from oxaloacetate and glyoxylate with H_2 or formate in the presence of ammonia (NH_4^+) under catalysis from Ni (10 mol% representing 640 ppm) or Pd (1 mol%, representing 64 ppm Pd) in pH 8 water at 22°C. Citroyl formate was not always detectable by ^1H NMR. Glutamate and hydroxy ketoglutarate were not detectable in the one-pot experiment.

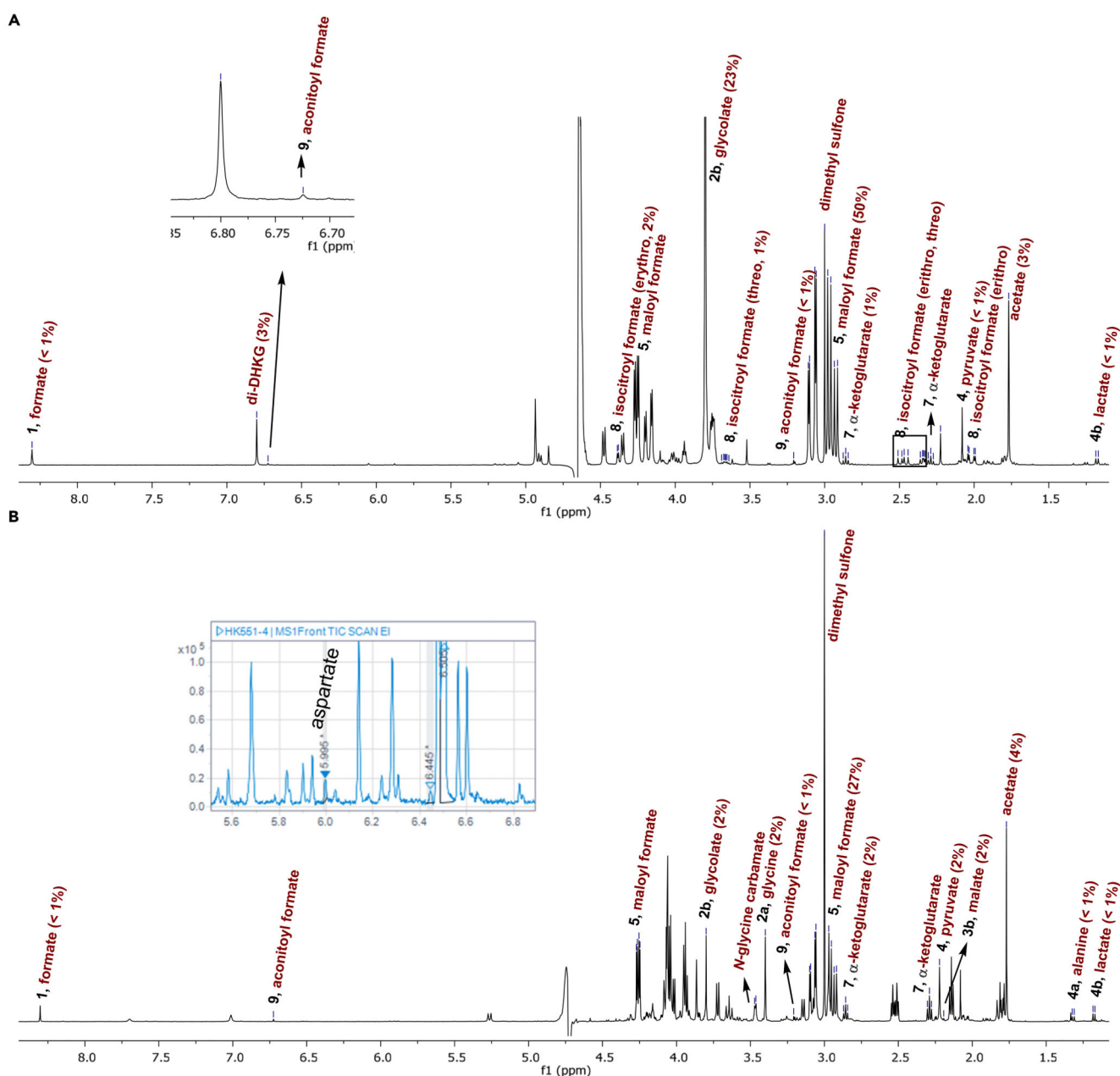


Figure 4. Nonenzymatic one-pot experiments in pH 8 water at 22°C starting from oxaloacetate (0.06 M), glyoxylate (0.12 M), and $\text{H}_2/\text{HCO}_3^-$ (5 bar/ 10 equiv) (A) ^1H NMR of the crude mixture resulting from the reaction of oxaloacetate and glyoxylate with sodium bicarbonate (10 equiv), under catalysis from Ni/ $\text{SiO}_2\text{-Al}_2\text{O}_3$ (10 mol%, 640 ppm relative to substrate). Reported yields were determined by quantitative ^1H NMR (see supplemental information, Figure 60; Table S16). 9 compounds of interest were detected in a combined yield of ~62% based on oxaloacetate and another 1 compound (glycolate) in 23% yield based on glyoxylate, assuming the reaction scheme in Figure 3. Malate was detectable by GC-MS (Figure S61). For the reaction with Pd, see Figure 59 and Table S15.

(B) ^1H NMR of the same one-pot experiment in the presence of ammonium NH_4^+ (NH_4HCO_3 , 10 equiv). Products of interest account for ~37% yield based on oxaloacetate with another 2 compounds (glycine and glycolate) accounting for ~3% based on glyoxylate. Aspartate was detectable in trace amounts by GC-MS in the case of Ni (Figure S58) but could additionally be observed in 5% yield by ^1H NMR in the case of Pd (Table S11; Figure S51). Control experiments can be found in Tables S17–S20 and Figures S62–S65.